

AD693313

CAMBRIDGE ACOUSTICAL ASSOCIATES, INC.

RESEARCH, DEVELOPMENT AND CONSULTING
IN ENGINEERING AND SCIENCE

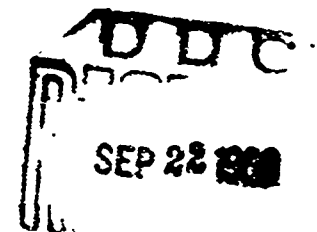
UNDERWATER SHOCKWAVE FOCUSING AT CAUSTICS:
Comparison of Theory and Experiment

David A. Sachs

31 August 1969

Final Report U-322-188
Prepared for
Field Projects Branch, Earth Sciences Division
Office of Naval Research - Code 418
Under Contract N00014-66-C-0110; NR 321-002/3-27-67

129 MOUNT AUBURN STREET, CAMBRIDGE, MASSACHUSETTS



40

UNDERWATER SHOCKWAVE FOCUSING AT CAUSTICS:

Comparison of Theory and Experiment

David A. Sachs

31 August 1969

Final Report U-322-188

Prepared for

Field Projects Branch, Earth Sciences Division

Office of Naval Research - Code 418

Under Contract N00014-66-C-0110; NR 321-002/3-27-67

Reproduction in Whole or in Part is Permitted
for Any Purpose of the United States Government

CAMBRIDGE ACOUSTICAL ASSOCIATES, INC
129 Mt. Auburn Street
Cambridge, Massachusetts 02138

ABSTRACT

The theory of shockwave focusing (developed by Silbiger¹) is employed in an attempt to predict the extent of focusing of explosive pulses at caustics as observed experimentally by Barash.²

Assuming a viscous medium and a physically reasonable model for the explosive pulse, an order of magnitude comparison with experiment is obtained. The omission of viscosity from the mathematical model leads to unacceptably large amplification at the caustic.

Table of Contents

	Page
Abstract.	i
List of Symbols.	iii
List of Figures.	vi
I. INTRODUCTION	1
II. COMPARISON OF THEORY AND EXPERIMENT.	2
A. Experimental Sound Speed Profile and Sound Sources . .	2
B. Mathematical Model of Experiment	2
1. Modeling the Source Pulse.	2
2. Modeling the Sound Speed Profile	7
3. Pressure Time History on Caustic: Inviscid Medium Model	11
4. Pressure Time History at Caustic: Viscous Medium Model.	16
III. CONCLUSIONS.	21
REFERENCES	30

List of Symbols

A	peak value of $F(t)$
AA	geometry-dependent factor appearing in theoretical expression for pressure time history in viscous medium
$AI(0)$	Airy function evaluated at zero argument
a	measure of rate of change of linear sound speed profile with z
c	speed of sound in water
$c(z)$	sound speed profile; variation in z -direction
c_0	speed of sound at $z=0$
FFP	geometry dependent but time independent portion of amplification factor (same for viscous or inviscid medium)
$F(t)$	time history of model source pulse
${}_1F_1(a;b;c)$	confluent hypergeometric function (Kummer's function)
$\tilde{F}(\omega)$	Fourier transform of model source pulse
f	frequency
$f(t, t_1, t_0)$	time-dependent but geometry-independent portion of amplification factor, viscosity absent
$f_v(t)$	time-dependent portion of amplification factor, viscosity present
$f(\xi, z)$	Hankel transform of pressure field for time-harmonic source
$H(t)$	time dependent function appearing in theoretical expression for pressure time history in viscous medium
i	$\sqrt{-1}$
$J_0(x)$	Bessel function of order zero and argument x
K	a geometry-dependent factor
k	$= \omega/c(0)$, wave number in water
k_{eff}	approximate wave number in viscous medium

$n(z)$	index of refraction
P_r	principal value
P_{iso}	empirical peak value of explosive pressure pulse in isovelocity water
$p(R,t)$	pressure time history
$p(r,z)$	pressure field for time-harmonic source
$p(r_c, z_c, t)$	computed time history of pressure pulse at observation point on caustic
$p(x,y,z,t)$	pressure field
R	range from location of sound source
R_c	horizontal range to origin of two-branched caustic
r_c	horizontal range to observation point on the caustic
$SGN(x)$	sign function of argument x
t	time
t_D	decay constant of explosive pulse
t_0	rise time of model source pulse $F(t)$
t_1	decay time of model source pulse $F(t)$ (if $t_0 \ll t_1$)
$W(\xi, z, r)$	phase function defined as $W = \xi r + \int_{z_T}^{z_0} \sqrt{n^2(z) - \xi^2} dz + \int_{z_T}^z \sqrt{n^2(z) - \xi^2} dz$
W_c	phase function defined by
	$W_c = \xi_c r_c + \int_{z_T}^{z_0} \sqrt{n^2(z) - \xi_c^2} dz + \int_{z_T}^{z_c} \sqrt{n^2(z) - \xi_c^2} dz$
W_c'''	third derivative with respect to ξ of W , evaluated at observation point on caustic
w	weight of pentolite explosive, in lbs
x,y,z	Cartesian coordinates

z_c	vertical distance of observation point on the caustic from $z=0$ axis
z_0	vertical distance of sound source from the origin
z, r	vertical and radial cylindrical coordinates
z_T	vertical coordinate of turning point for the ray characterized by ξ [in $W(\xi, z, r)$] or ξ_c (in W_c)
α	$= v/2c^3(o)$
β	$= vW_c/2c^3(o)$
$\Gamma(x)$	gamma function of argument x
∇^2	Laplacian operator
$\delta(x), \delta(y), \delta(z)$	Dirac delta functions
$ e $	viscous damping factor
η	coefficient of bulk viscosity
μ	coefficient of shear viscosity
ξ	sine of the angle with respect to the vertical at which the ray passing through the observation point leaves the source
ξ_c	sine of the angle with respect to the vertical at which the ray touching the caustic at the observation point leaves the source
ρ	density of water
ν	kinematic viscosity coefficient
ω	circular frequency

List of Figures

	Page
Fig. 1. Experimental sound velocity profile.	22
Fig. 2. Experimental ray diagram	23
Fig. 3. Mathematical model of source pulse	24
Fig. 4a. Mathematical model of bilinear sound speed profile . .	25
Fig. 4b. Ray diagram for mathematical model of bilinear profile	26
Fig. 5. Mathematical prediction of pressure pulse shape: no viscosity, rise-time t_0	27
Fig. 6. Experimental pressure time history	28
Fig. 7. Theoretical pressure time history for a viscous medium	29

I. INTRODUCTION

Because the speed of sound varies from point-to-point in most bodies of water, shockwaves propagating under water do not travel in straight lines but rather in curved paths. Under certain conditions and in certain regions the paths converge, or focus, and sound energy which had previously been distributed over a large volume of water is concentrated into a small volume. Regions in which this effect occurs are called convergence zones. Convergence zones consist of a point, line or surface - called the caustic - where the focusing is maximum, surrounded by a narrow region in which the focusing effect diminishes with distance from the caustic.

For submerged sources of explosive sound, the pressure pulses appearing at the caustics display marked amplification of the peak value and distortion of the waveform.

A theory to describe the propagation and focusing of transient pulses in convergence zones has been proposed by Silbiger.¹ The theory is based on the fundamental assumptions of the validity of linear acoustics and the absence of viscosity in the propagating medium. Modifications to incorporate viscous effects into the theory can be made and are discussed in a later part of this report. Non-linear effects can also be included in the theory; however, they are not considered in this report.

By making a series of mathematical approximations, the theory can be shown to reduce to the results of geometric acoustics, in regions off caustics and not in shadow zones. Through a modification of geometric acoustics, the theory yields predictions of the pressure on the caustic itself and in the shadow zone near the caustic.¹

The goal of this report is to report results of a numerical comparison of the Silbiger theory with the experimental results of Barash.²

The numerical comparison with experiment indicates that an order of magnitude prediction of the peak amplification of a focused pulse is obtained assuming a viscous medium and zero rise time source pulse.

II. COMPARISON OF THEORY AND EXPERIMENT

A. Experimental Sound Speed Profile and Sound Sources

Barash² observed the focusing of underwater shockwaves produced by detonating pentolite explosives in a quarry with a sound speed profile as shown in Fig. 1. In one of his experiments the sound source was placed at a depth of 50 ft for which the sound rays (determined by Snell's law) are shown in Fig. 2. A caustic surface is evident. Barash observed the pressure pulse produced at the caustic by the detonation.

We shall be concerned with reproducing theoretically the experimental results for a particular combination of experimental parameters: charge weight, 0.122 lb; charge depth, 50 ft; and a horizontal range (to the observation point on the caustic) of 300 ft, at which the caustic depth was 29.2 ft.

B. Mathematical Model of Experiment

1. Modeling the Source Pulse

A fundamental assumption of the Silbiger theory of shockwave focusing is that non-linear effects are unimportant. These can arise from large amplitude pressure waves so we chose to consider the smallest explosive weight experimentally employed (0.122 lb) in the expectation that linear acoustics theory will be valid.

The pressure pulse produced in the vicinity of a submerged explosive is usually said to have a negligible rise time and an exponential decay, the decay constant and peak value being functions of the charge weight and type, and the range.³ For pentolite charges in a non-refractive medium, we have

$$p(R,t) = 2.25 \times 10^4 \left(\frac{w}{R} \right)^{1.13} e^{-\frac{(t-R/c)}{t_D}} \left(t \geq \frac{R}{c} \right) \quad \left(\frac{lb}{in.^2} \right)$$

$$= 0 \quad \left(t < \frac{R}{c} \right) \quad (1)$$

where w is the charge weight in pounds, R is the range in feet and c is the velocity of sound. t_D , the decay constant, is given by

$$t_D = 58 w^{1/3} \left(\frac{w}{R} \right)^{-0.22} \quad (\text{micro-secs}) \quad (2)$$

A "negligible" rise time presumably means a rise time much smaller than experimental equipment can detect. As of yet, investigators in the field of underwater detonations have not achieved a measurement of the rise time close to the explosion; the generally quoted (and used) value is zero. Clearly there is some non-zero yet very small rise time; about the only quantitative statement that can be made is that the rise time must be much shorter than an observable decay time.

In Silbiger's notation, the pressure radiated by a transient source into an inhomogeneous medium obeys the following wave equation:¹

$$\nabla^2 p(x,y,z,t) - \frac{1}{c^2(z)} \frac{\partial^2}{\partial t^2} p(x,y,z,t) = - \delta(x)\delta(y)\delta(z) F(t) \quad (3)$$

where close to the source (located at the origin), the pressure is an initially spherical wave of the form

$$\begin{aligned} p(R,t) &= \frac{F(t-R/c)}{4\pi R} & (t \geq R/c) \\ &= 0 & (t < R/c) \end{aligned} \quad (4)$$

and R is the range from the source, while c is the velocity of sound in the neighborhood of the source.

For mathematical convenience, we model the source pulse [denoted by $F(t)$] as a linearly increasing line segment followed by a linearly decreasing line segment. Thus, the model source pulse is described by the equations

$$\begin{aligned} F(t) &= 0 & t < 0 & \quad (a) \\ &= A \frac{t}{t_0} & 0 \leq t \leq t_0 & \quad (b) \\ &= \frac{A(t-t_1)}{(t_0-t_1)} & t_0 \leq t \leq t_1 & \quad (c) \\ &= 0 & t \geq t_1 & \quad (d) \end{aligned} \quad (5)$$

and is shown in Fig. 3.

Turning our attention back to Eqs. 1 and 2, we note that the exponents 1.13 and -0.22 appearing in Eqs. 1 and 2 would be replaced by unity and zero, respectively, in an absorption-free linear fluid, corresponding to spherical spreading and a time constant independent of distance.³ The peculiar exponents appear due to a combination of non-linear effects of the water medium and viscous attenuation. We make the assumption that both these effects accumulate with distance from the source so that the exponents 1.13 and -0.22 can be replaced by one and zero, respectively, in the neighborhood of the source.

With this assumption, we determine A by setting the peak value of Eq. 4 equal to the peak value of (the modified form of) Eq. 1, i.e.,

$$\frac{A}{4\pi R} = 2.25 \times 10^4 \frac{w^{1/3}}{R}$$

or

$$A = 4\pi (2.25 \times 10^4) w^{1/3}$$

Setting the exponent -0.22 in Eq. 2 equal to zero, the decay time in the neighborhood of the source is then

$$t_D = 58 w^{1/3} \quad (\text{micro-sec})$$

or, for $w = 0.122$ lbs,

$$t_D = 2.87 \times 10^{-5} \text{ secs}$$

For convenience, we will henceforth take t_D as 10^{-5} secs; it will turn out that the theoretical predictions are only weakly dependent on t_D .

Note from Eq. 1 that, for small values of $(t-R/c)/t_D$, we have

$$\begin{aligned} e^{\frac{(t-R/c)}{t_D}} &\approx 1 - \frac{(t-R/c)}{t_D} \\ &= \frac{t_D - (t-R/c)}{t_D} \end{aligned}$$

Comparing the above with Eq. 5c, we see that if the rise time of the model t_0 is such that $t_0 \ll t_1$, as it should be physically, Eq. 5c will approximate the (early times) linear portion of the decay of Eq. 1 if

$$t_D = t_1$$

and

$$\frac{(t-R/c)}{t_D} \ll 1$$

or

$$(t-R/c) \ll 10^{-5} \text{ secs.}$$

That is, the model source pulse will accurately represent the decay of (the modified form of) Eq. 1 only for a time interval up to 10^{-6} secs or so after occurrence of the peak value.

In the absence of caustics and viscosity, the pressure predicted by the Silbiger theory is, aside from a multiplicative amplitude factor dependent on geometry, a time delayed replica of the source pulse.

After a pulse has propagated through a caustic, the pressure time history is of the form⁴

$$p(x,y,z,t) = K \text{ Pr} \int_{-\infty}^{+\infty} \frac{F(T)}{T-t} dT$$

where K is a geometry-dependent factor, $F(T)$ is the time history of the source pulse, t is the time of observation and Pr denotes principal value.

From the definition of the principal value integral, it can be shown that the pressure field will diverge at certain times if $F(T)$ has any discontinuities. Therefore, in the absence of viscosity, the model source pulse must have non-zero rise and decay times, lest the theory predict infinite values for the pressure in the presence of caustics.

It is shown in a later section that the effects of viscosity can be incorporated into the theory by the introduction of a complex propagation constant. Expressed as a Fourier integral over the Fourier spectrum $\tilde{F}(\omega)$ of the source pulse, the pressure appears as

$$p(x,y,z,t) = K \int_{-\infty}^{+\infty} e^{-i\omega t - |\epsilon|\omega^2 - \pi\omega/(2|\omega|)} \tilde{F}(\omega) d\omega$$

where $\omega=2\pi f$ is the circular frequency. The presence of the exponential damping factor can be shown to insure a finite pressure at all times, even in the presence of discontinuities in $F(T)$, provided that $F(T)$ is finite and is of finite duration. Thus, if the medium is assumed to be viscous, the model source pulse may have vanishing rise and/or decay times.

As it is well known that sound waves propagating in water suffer viscous attenuation,⁵ two models of the water medium are considered for the sake of comparison: one with viscosity included, the other without.

2. Modeling the Sound Speed Profile

The sound speed profile is modeled by the bilinear profile shown in Fig. 4a, along with its associated ray diagram (Fig. 4b) corresponding to the experimental sound source location. The model profile neglects the isovelocity segment of the experimental profile which originates at the water surface, as well as the quarry bottom, walls and water surface.

The caustic in the inhomogeneous layer corresponds to the experimental caustic. The second caustic extends to infinite distances only because the surface isovelocity layer is omitted in the model. If the surface isovelocity layer were included, consideration of the permissible ray paths would show that the second caustic would only extend a short distance from the common

point of origin of the two caustics. Some ambiguity is introduced by the omission. On the one hand, in the geometrical acoustics limit the pressure pulse is determined by sound which has traversed ray paths lying entirely within the sloping portion of the actual profile, and these critical ray paths are reproduced in the bilinear model. However, experimentally, a signal with a distinct beginning is observed to precede the onset of the caustic-focused pulse. This precursor signal most likely arises from sound which has propagated, at least in part, along the intersection between the surface isovelocity layer and the sloping portion of the actual profile.⁶ The bilinear model will be unable, consequently, to predict this signal and, indeed, some uncertainty in the interpretation of the experimental records is the result.

The omission of the bottom, walls and water surface is justified since a pulse reflected from any of these surfaces will arrive at the observation point much later than the caustic-focused pulse, and in practice, produces an easily identifiable trace in the experimental records.

The velocity profile of the bilinear model is described mathematically by the relations

$$\begin{aligned} c(z) &= c_0 (1-az) \quad z \leq 0 \\ &= c_0 \quad z > 0 \end{aligned}$$

The Silbiger theory then contains three parameters: the gradient (slope) of the linearly increasing segment (denoted by a), the distance of the source from the origin (denoted by z_0) and the sound speed at the origin (c_0).

These parameters are fixed by requiring that the model reproduce (i) the experimental vertical distance between the source and point of observation on the caustic (at the experimental horizontal range), (ii) the experimental horizontal range (from the source) of the origin of the caustics, and (iii) the average sound speed of the lower isovelocity segment of the experimental profile. A reasonable fit of the experimental situation was obtained with

$$z_0 = 20.8 \text{ feet}$$

$$a = 2.707 \times 10^{-3} (\text{ft})^{-1}$$

$$c_0 = 4715 \text{ ft/sec}$$

Smaller values of the parameter a yielded significant disagreement with the experimental range to the caustic origin; larger values produce a large discrepancy with the experimental vertical distance between source and caustic. A comparison between the model and the experiment is shown in Table 1, along with some other choices of model parameters to provide a comparison. The quantity $(z_0 - z_c)$ is the vertical distance between the source and the caustic. R is the horizontal range.

Note that the horizontal range to the origin of the caustic is not well defined experimentally (see Table 1 and Fig. 2). According to the bilinear model, $z_0 - z_c$ should decrease monotonically as a function of horizontal range, whereas in Table 1 the experimental value of $z_0 - z_c$ is non-monotonic for the closest ranges. Our choice of model parameters yields a range of 227.7 feet.

Table 1

VERTICAL SOURCE-CAUSTIC DISTANCE (FT) VERSUS HORIZONTAL RANGE (FT)

EXPERIMENT		BILINEAR MODEL							
		$z_0 = 20.8 \text{ ft}$ $a = 2.707 \times 10^{-3} \text{ ft}^{-1}$		$z_0 = 20.0 \text{ ft}$ $a = 2.707 \times 10^{-3} \text{ ft}^{-1}$		$z_0 = 18.0 \text{ ft}$ $a = 2.024 \times 10^{-3} \text{ ft}^{-1}$		$z_0 = 17.0 \text{ ft}$ $a = 1.341 \times 10^{-3} \text{ ft}^{-1}$	
R	$z_0 - z_c$	R	$z_0 - z_c$	R	$z_0 - z_c$	R	$z_0 - z_c$	R	$z_0 - z_c$
189.5	29.1								
193.1	28.6								
209.8	27.8								
210.1	28.0								
215.8	27.1								
		227.7	23.3						
232.2	25.7	231.7	23.2	234.3	22.0				
243.5	24.9	243.7	22.8	244.3	21.8	245.0	20.2		
257.6	24.1	257.7	22.5	259.3	21.5	258.0	19.8		
275.3	23.1	275.7	22.2	274.3	21.3	275.0	19.5	292.6	19.1
298.0	22.1	297.7	21.9	299.3	21.0	298.0	19.2	297.6	19.0
331.9	20.0	332.0	21.7			332.0	18.9	332.0	18.3
378.1	17.6	378.0	21.4	380.0	20.6	378.0	18.6	378.0	17.9
389.9	16.7	390.0	21.4	390.0	20.5	380.0	18.6	390.0	17.9
416.5	15.0	400.0	21.4	400.0	20.5	400.0	18.6	400.0	17.8

3. Pressure Time History on Caustic: Inviscid Medium Model

For points on the caustic (in a non-viscous medium), the time history of the pressure is given by⁷

$$p(r_c, z_c, t) = \frac{1}{8\pi^2} \left[\frac{2\pi c(o)^{-1/3} \xi_c}{r_c [n^2(z_c) - \xi_c^2]^{\frac{1}{2}} [n^2(z_o) - \xi_c^2]^{\frac{1}{2}}} \right]^{\frac{1}{2}} \left(\frac{1}{2} |W_c''| \right)^{-1/3} Ai(o) \cdot \int_{-\infty}^{+\infty} \mathcal{F}(\omega) |\omega|^{1/6} \exp\{i\omega[W_c/c(o) - t - \frac{\pi}{4}|\omega|]\} d\omega \quad (6)$$

where r_c and z_c are the cylindrical coordinates of the point of observation on the caustic, $c(o)$ is the sound speed at the origin, ξ_c is the sine of the angle with respect to the vertical at which the ray touching the caustic at the observation point leaves the source, $n(z_c)[n(z_o)]$ is the index of refraction at the caustic (source), W_c'' is the third derivative with respect to ξ of the phase function $W(\xi, z, r)$ evaluated at ξ_c, z_c, r_c , where

$$W(\xi, z, r) = \xi r + \int_{z_r}^{z_c} \sqrt{n^2(z) - \xi^2} dz + \int_{z_r}^z \sqrt{n^2(z) - \xi^2} dz$$

and z_r is the turning point for the ray characterized by ξ , $Ai(o)$ is the Airy function evaluated at zero argument, $\mathcal{F}(\omega)$ is the Fourier transform of $F(t)$, defined by the relation

$$\mathcal{F}(\omega) = \int_{-\infty}^{+\infty} F(t) e^{i\omega t} dt$$

and for the model source pulse (Fig. 3) is given by

$$\mathcal{F}(\omega) = \frac{A}{\omega^2} \left[\frac{(e^{i\omega t_o} - 1)}{t_o} + \frac{e^{i\omega t_1}}{t_o - t_1} - \frac{e^{i\omega t_o}}{t_o - t_1} \right] \quad (7)$$

ω is the circular frequency, W_c is $W(\xi_c, z_c, r_c)$ and t is the time. Using Eq. 7, the pressure can be written in closed form:

$$P(r_c, z_c, t) = \frac{1}{4\pi} \left(\frac{1}{2} \left| W_c'' \right| \right)^{-1/3} \left[\frac{2\pi \xi_c c(o)^{-1/3}}{r_c [n^2(z_c) - \xi_c^2]^{\frac{1}{2}} [1 - \xi_c^2]^{\frac{1}{2}}} \right]^{\frac{1}{2}} Ai(o) \\ A \frac{3}{5} \Gamma\left(\frac{1}{6}\right) \left[\frac{t_1}{t_o(t_o - t_1)} \left| t - \frac{W_c}{c(o)} - t_o \right|^{5/6} \{(\sqrt{3}-1 + \text{SGN} \right. \\ \left. (t - \frac{W_c}{c(o)} - t_o)(\sqrt{3}+1)\} + \frac{1}{t_o} \left| t - \frac{W_c}{c(o)} \right|^{5/6} \{(\sqrt{3}-1) + \text{SGN}(t - \frac{W_c}{c(o)})(\sqrt{3}+1)\} \right. \\ \left. - \frac{1}{(t_o - t_1)} \left| t - \frac{W_c}{c(o)} - t_1 \right|^{5/6} \{(\sqrt{3}-1) + \text{SGN}(t - \frac{W_c}{c(o)} - t_1)(\sqrt{3}+1)\} \right] \quad (8)$$

where $\text{SGN}(x) = 1 \quad x > 0$
 $= -1 \quad x < 0$

The experimental data of Barash is presented not in terms of the pressure directly, but rather in terms of the ratio of the observed pressure pulse to the peak value of the pressure pulse which would be observed if the water had a uniform velocity. This ratio is called the amplification factor. For isovelocity water, the peak value of the pressure pulse would be⁸

$$P_{iso} = 2.25 \times 10^4 \left(\frac{w^{1/3}}{\sqrt{r_c^2 + (z_c - z_o)^2}} \right)^{1.13} \frac{1b}{in^2}$$

where w is the weight (in pounds) of the explosive and r_c , z_c and z_o are measured in feet.

Denoting the last bracketed expression on the right hand side of Eq. 8 by $f(t, t_1, t_0)$, the amplification factor can be written as

$$\frac{p(r_c, z_c, t)}{P_{iso}} \cong FPP \cdot f(t, t_1, t_0) \quad (9)$$

The factor FPP is determined by the location of the point of observation and the parameters of the bilinear model. FPP, as a function of the model parameters, is given in Table 2. The horizontal range (R_c) to the caustic origin is also shown. FPP is strongly dependent on the slope (a). R_c varies with both z_0 and a . As mentioned before, the first set of parameters offers the most reasonable fit to the experimental caustic curve.

The maximum value of the function $f(t, t_1, t_0)$ is shown in Table 3 along with the corresponding maximum value of the amplification factor, for a series of values of t_1 and t_0 . The observed maximum amplification factor is 4.95. All the predicted values are too high.

If the precursor pressure and the caustic-focused pressure combine additively to yield the experimental record, the experimental amplification factor would be reduced to about 3.3. It is not clear, however, if this interpretation is correct but a theoretical study of precursors is in progress. In any case, the predicted values will still be too high.

The function $f(t, t_1, t_0)$ is shown in Fig. 5. Values of $f(t, t_1, t_0)$ for time intervals larger than about 10^{-6} seconds on either side of the origin are not expected to be accurate because: (1) the model source pulse is valid only up to times of 10^{-6} seconds or so, and (2) the high-frequency approximations made in the theory itself. These latter limitations have not been

Table 2

FPP AS FUNCTION OF BILINEAR MODEL PARAMETERS

$a \text{ (ft}^{-1}\text{)}$	$z_0 \text{ (ft)}$	$c(0) \text{ (ft/sec)}$	FPP	$R_c \text{ (ft)}$
2.707×10^{-3}	20.8	4715	.258	227.8
2.024×10^{-3}	18.0	4714	.272	245.0
1.341×10^{-3}	17.0	4714	.402	292.6

Table 3

MAXIMUM VALUES OF $f(t, t_1, t_0)$ AND THE AMPLITUDE FACTOR
AS FUNCTIONS OF t_1 AND t_0

$t_1(\text{sec})$	$t_0(\text{sec})$	$f(t, t_1, t_0)_{\text{MAX}}$	MAXIMUM AMP FACTOR
10^{-5}	10^{-7}	37.37	9.6
10^{-5}	10^{-8}	61.22	15.8
10^{-5}	10^{-9}	95.94	24.7
10^{-4}	10^{-6}	25.4	6.5
10^{-4}	10^{-8}	69.2	17.7
10^{-4}	2.1×10^{-17}	2091	539
10^{-4}	3×10^{-18}	3341	860

investigated thoroughly enough to justify a discussion of them here. However, a study of the limitations of the caustic boundary layer formulae is in progress. The slowly rising signal occurring prior to $t=0$ has no definite time of onset and may be associated with the high frequency nature of some of the approximations employed in the theory. Its significance has yet to be studied in detail.

The experimentally observed time history (of the amplification factor) is shown in Fig. 6. The precursor signal precedes the actual focused pulse. The theory, as presently formulated, cannot predict this signal.

The details of the experimental record are, to some extent, unreliable in the sense that a sudden rise in pressure was recorded with a 10 micro-second rise time.² Hence, although it appears in Fig. 6 as though the experimentally observed rise and decay times of the focused pulse are both on the order of 10^{-5} secs, they may in fact be shorter than that.

At any rate, we can conclude from Table 3 that the rise time required by the theory to reproduce the experimental peak amplification factor is unrealistically large, since it must be longer than 10^{-7} secs, for $t_1 = 10^{-5}$ secs.

4. Pressure Time History at Caustic: Viscous Medium Model

The time dependent wave equation, including viscosity, is given by⁹

$$\begin{aligned} \nabla^2 p(x,y,z,t) + \frac{v}{c^2(z)} \frac{\partial}{\partial t} \nabla^2 p(x,y,z,t) - \frac{1}{c^2(z)} \frac{\partial^2}{\partial t^2} p(x,y,z,t) \\ = - \delta(x)\delta(y)\delta(z) \left[F(t) + \frac{v}{c^2(o)} \frac{\partial}{\partial t} F(t) \right] \end{aligned}$$

where ν is the kinematic viscosity coefficient defined as

$$\nu = \frac{\eta + \frac{4}{3} \mu}{\rho}$$

and

η = coefficient of bulk viscosity

μ = coefficient of shear viscosity

ρ = density

For a sinusoidal source ($e^{-i\omega t}$ time dependence) of strength $\tilde{F}(\omega)$, the viscous wave equation reduces to

$$\nabla^2 p + \frac{k^2 n^2(z)}{[1 - \frac{i\omega\nu}{c^2(z)}]} p = -\tilde{F}(\omega) \delta(x)\delta(y)\delta(z) \quad (10)$$

If

$$\left| \frac{\omega\nu}{c^2(z)} \right| \ll 1 \quad (11)$$

and the variation of $c(z)$ in the spatial domain of interest is small enough, then in the factor $[1 - \frac{i\omega\nu}{c^2(z)}]^{-1}$, $c(z)$ may be replaced by $c(0)$ and an effective propagation constant defined as follows

$$k_{\text{eff}} = \frac{k}{\sqrt{1 - \frac{i\omega\nu}{c^2(0)}}}$$

$$\approx k[1 + i \frac{k\nu}{2c(0)}]$$

Introducing the Hankel transform pair

$$f(\xi, z) = \int_0^\infty p(r, z) J_0(k_{\text{eff}} \xi r) r dr \quad (12)$$

$$p(r, z) = \int_0^{\infty} f(\xi, z) J_0(k_{\text{eff}} \xi r) k_{\text{eff}}^2 \xi d\xi \quad (13)$$

the transform of Eq. 10 becomes

$$\frac{d^2}{dz^2} f(\xi, z) + k_{\text{eff}}^2 [n^2(z) - \xi^2] f(\xi, z) = -\frac{F(\omega)}{2\pi} \delta(z) \quad (14)$$

Proceeding from Eqs. 12 and 13, the development of the caustic boundary layer formalism proceeds as in the non-viscous case, the only difference being the appearance of k_{eff} instead of k .

The pressure time history on the caustic is then given by

$$p(r_c, z_c, t) = \frac{(AA)Ai(0)}{2\pi} [e^{-i\pi/4} \int_0^{\infty} d\omega f(\omega) e^{i\omega[W_c/c(0)-t]-i\alpha\omega^2} \omega^{1/6} + \text{complex conjugate}]$$

where

$$AA \equiv \frac{1}{4\pi} \left[\frac{2\pi \xi_c c(0)^{-1/3}}{r_c (n^2(z_c) - \xi_c^2)^{1/2} (n^2(z_0) - \xi_c^2)^{1/2}} \right]^{1/2} \left(\frac{1}{2} |\xi_c^{\omega}| \right)^{-1/3}$$

and

$$\alpha \equiv \frac{v}{2c^3(0)}$$

For the model source pulse, the pressure time history is given by

$$p(r_c, z_c, t) = \frac{(AA) \cdot Ai(0) \cdot A \cdot \sqrt{2}}{2\pi} \left\{ \frac{t_1}{t_0(t_1 - t_0)} H\left[\frac{W_c}{c(0)} - t + t_0\right] - \frac{1}{t_0} H\left[\frac{W_c}{c(0)} - t\right] - \frac{1}{(t_1 - t_0)} H\left[\frac{W_c}{c(0)} - t + t_1\right] \right\} \quad (15)$$

where

$$\begin{aligned}
 H(t) \equiv & -\frac{6}{5} \beta^{-7/12} \Gamma(7/12) {}_1F_1\left(\frac{7}{12}; \frac{1}{2}; -\frac{|t|^2}{4\beta}\right) \\
 & + t\beta^{-13/12} {}_1F_1\left(\frac{13}{12}; \frac{3}{2}; -\frac{|t|^2}{4\beta}\right) \\
 & + \frac{3}{5} t[\beta^{-1/12} \Gamma(1/12) {}_1F_1\left(\frac{1}{12}; \frac{1}{2}; -\frac{|t|^2}{4\beta}\right) \\
 & - t\beta^{-7/12} \Gamma(7/12) {}_1F_1\left(\frac{7}{12}; \frac{3}{2}; -\frac{|t|^2}{4\beta}\right)]
 \end{aligned}$$

and

$$\epsilon \equiv \frac{v W_c}{2c^3(o)}$$

Using the asymptotic form of ${}_1F_1$ valid for $|t|^2/4\beta \gg 1$, it can be verified that: (a) Eq. 15 reduces to the non-viscous pressure in the limit $\beta \rightarrow 0$ (no viscosity) and (b) Eq. 15 reduces to the non-viscous pressure in the limit to $|t_0|^2/4\beta \gg 1$, $|t_1|^2/4\beta \gg 1$. The first limit provides a check on Eq. 15. The second limit implies that for sufficiently long rise and decay times, viscous attenuation has no effect on the pressure time history. This is reasonable since long rise and decay times means there is very little high frequency content in the Fourier spectrum of $F(t)$. This being the case, it is immaterial whether the high frequency components get damped out or not. (Recall that viscous attenuation goes as $e^{-\text{constant} \cdot \omega^2}$.)

A function analogous to $f(t, t_1, t_0)$ of Eq. 9 can be defined for the viscous model. For a model source pulse with zero rise time and $t_1 = 10^{-5}$ seconds, the function [denoted by $f_v(t)$] is shown in Fig. 7. The viscosity

related parameters are for fresh water:⁵ $\mu = 0.01$ g/cm-sec and $\eta = 2.81$ μ . $c(0)$ was taken as 1.5×10^5 cm/sec and W_c as 300 ft, the distance along the ray path to the point of observation. The amplification is then taken as $f_v(t)$ times FPP as defined in Eq. 9.

As in the non-viscous case, the computed time history has a limited time domain of validity. A numerical evaluation of the inequality of Eq. 11 shows that $\omega v/c^2(z)$ is on the order of 0.1 for a frequency of 10^{10} Hz. Therefore the computed time history should be unreliable for times shorter than about 10^{-10} seconds. As mentioned before in connection with the inviscid medium, the model source pulse becomes unreliable for times longer than 10^{-6} seconds or so. Therefore, the computed time history should become erroneous for times (beyond the origin) of the same magnitude. In addition, the theory is based on a high frequency approximation which will render the time history reliable for only a short time interval after onset. However, a quantitative description of this source of error is not yet available.

For the model source pulse (Fig. 3) with $t_0=0, t_1=10^{-5}$ secs, the theoretical peak amplification factor is 6.1, as compared to the experimental value of 4.95.

If the precursor pressure and the caustic-focused pressure combined additively to yield the experimental record, then the experimental amplification factor would be about 3.3.

In either case, the predicted value is too high by 20 to 100 percent. If a non-zero rise time in the model source pulse were assumed, the theoretical prediction should decrease. It is possible that a more reasonable prediction could be made with a non-zero yet physically reasonable rise time, but this has not been attempted.

III. CONCLUSIONS

Assuring a source with finite rise time and an inviscid medium, the computed amplification factors are much too high if a physically acceptable rise time is assumed.

For a source with zero rise time radiating into a viscous medium, the theoretically computed amplification factor is 20 percent to 100 percent too high. A non-zero rise time might reduce the discrepancy.

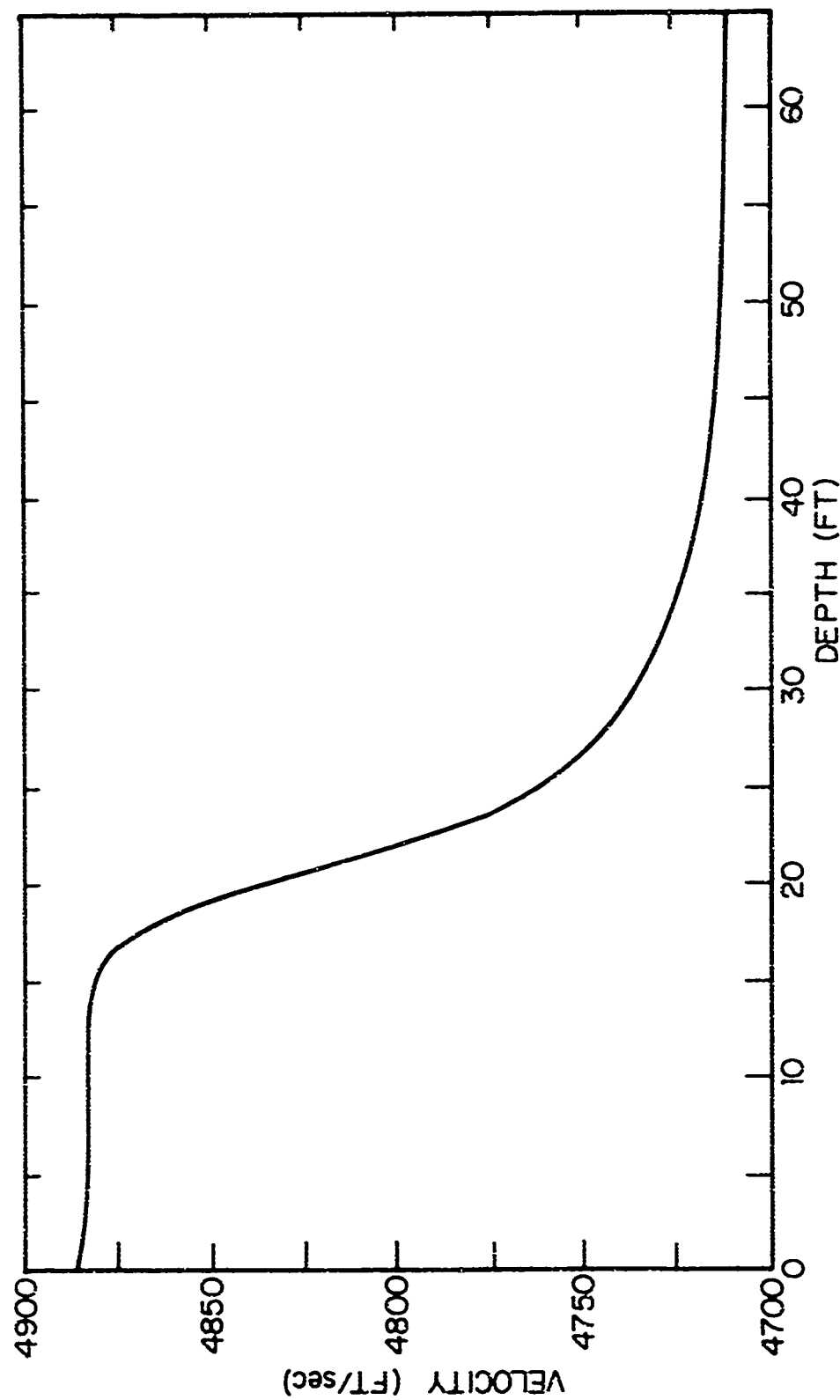


Fig. 1. Experimental sound velocity profile. (Courtesy of R. H. Barash and R. Tarun, U.S. Naval Ordnance Laboratory.)

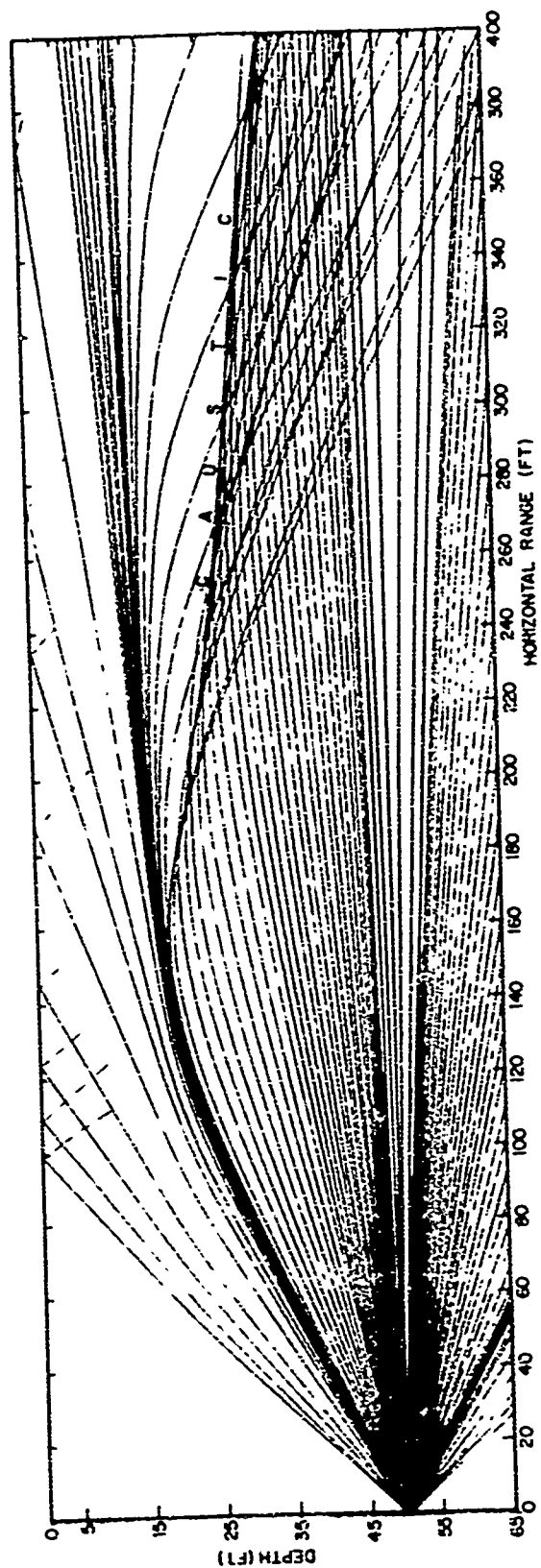


Fig. 2. Experimental ray diagram. (Courtesy of R. M. Barash and R. Thrun, U. S. Naval Ordnance Laboratory.)

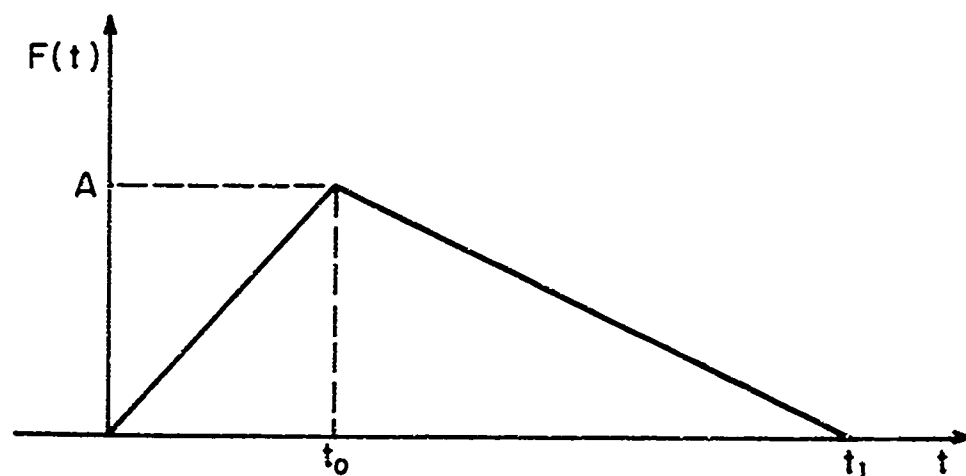


Fig. 3. Mathematical model of source pulse.

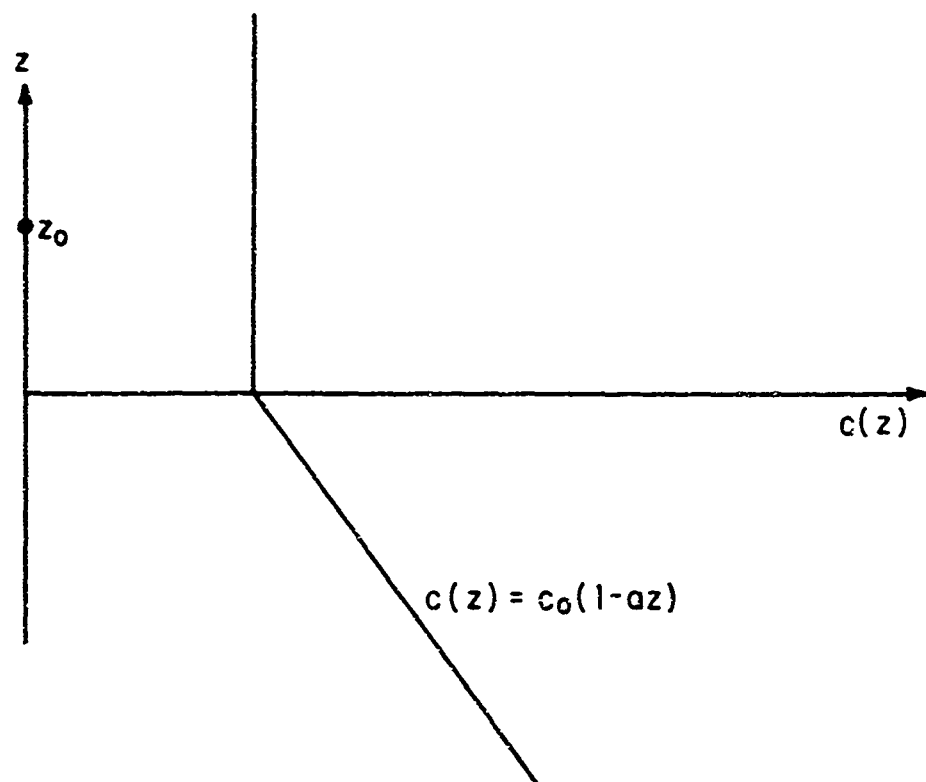


Fig. 4a. Mathematical model of bilinear sound speed profile.

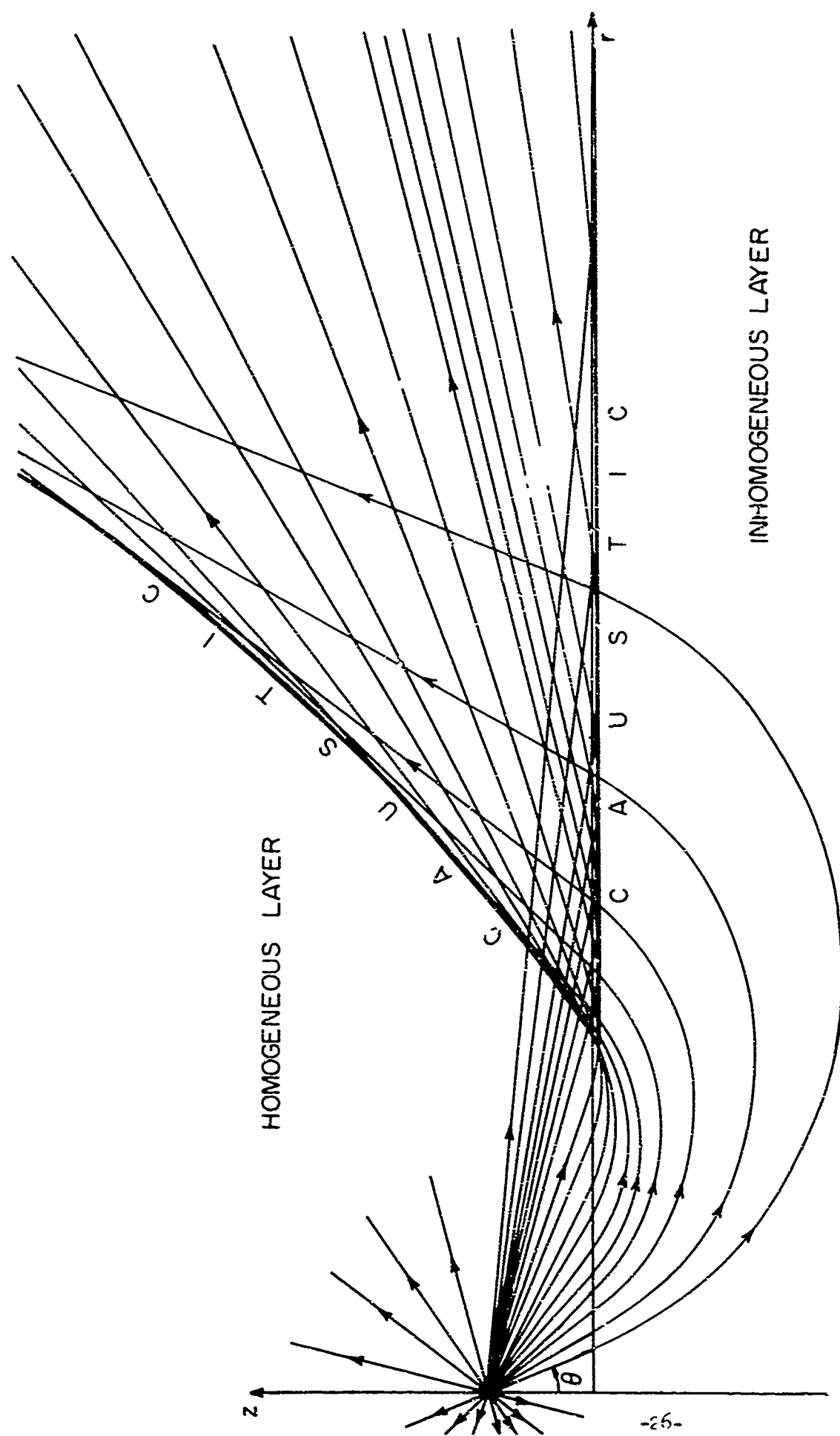


Fig. 4b. Ray diagram for mathematical model of bilinear profile. z increase with depth. Horizontal caustic is the one observed experimentally by Varsh, \bar{z}

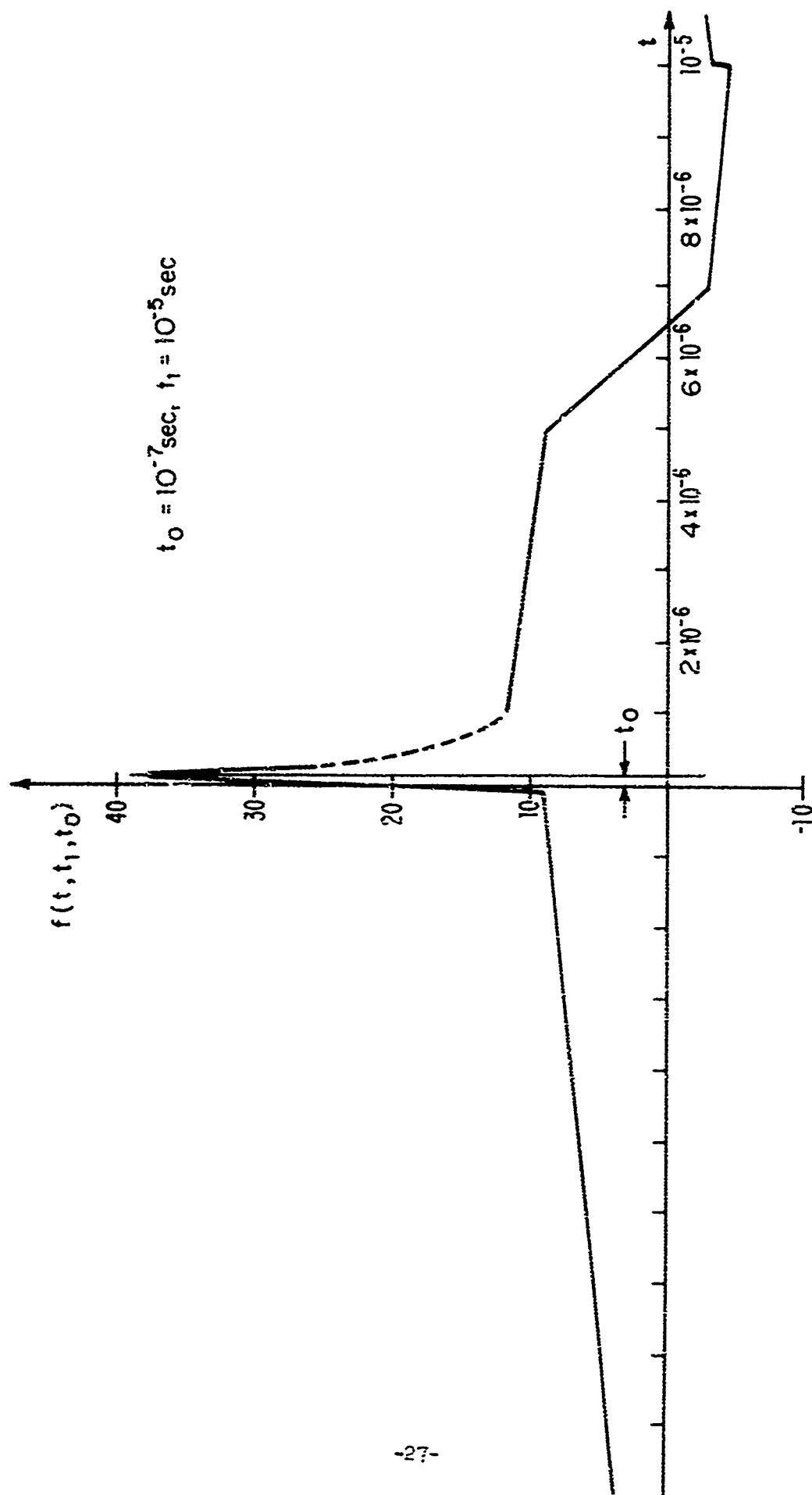


Fig. 2. Mathematical prediction of pressure pulse shape: no viscosity, rise-time t_0 .

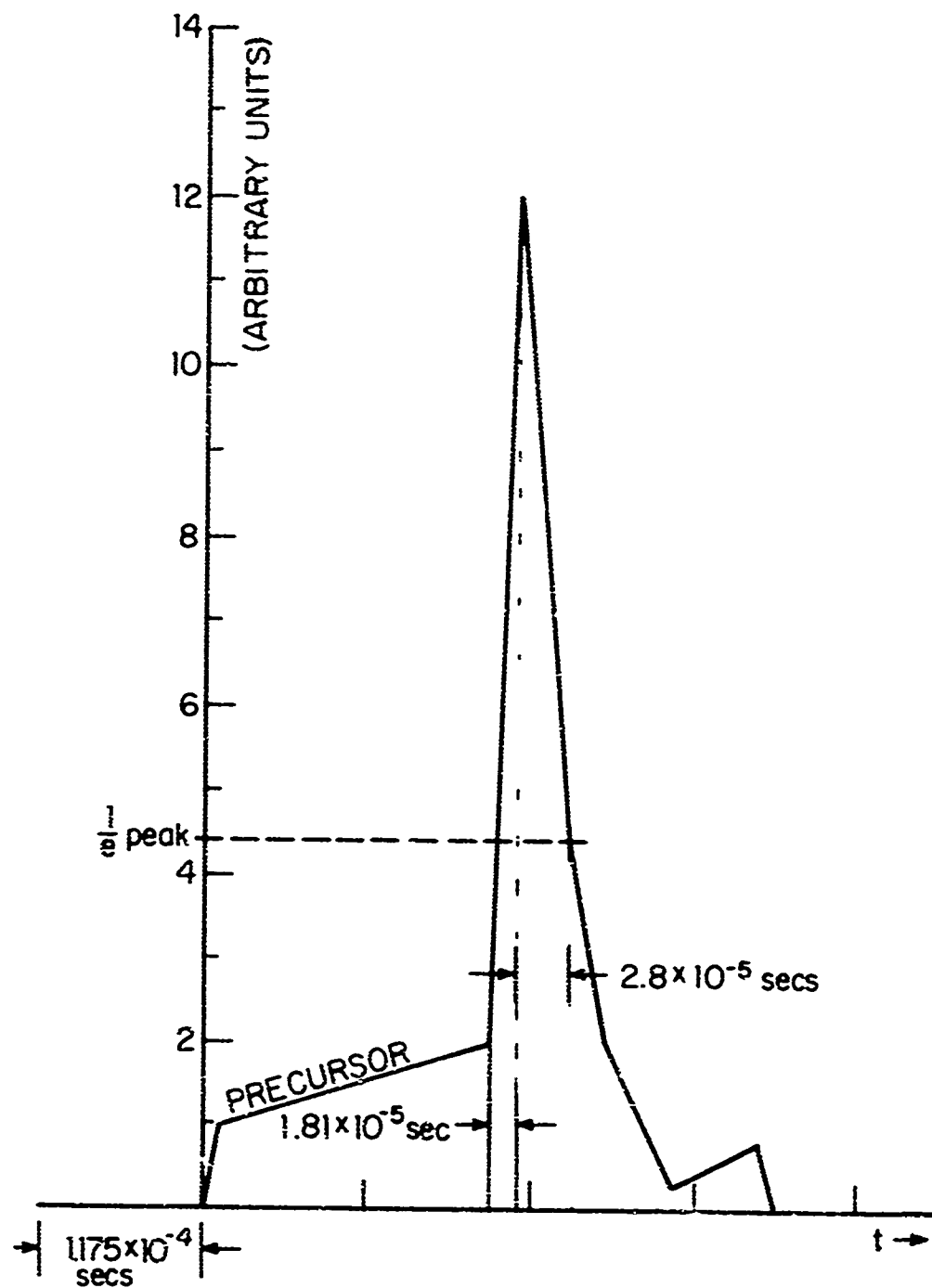


Fig. 6. Experimental pressure time history.
(Based on the data of R. M. Barash.²)

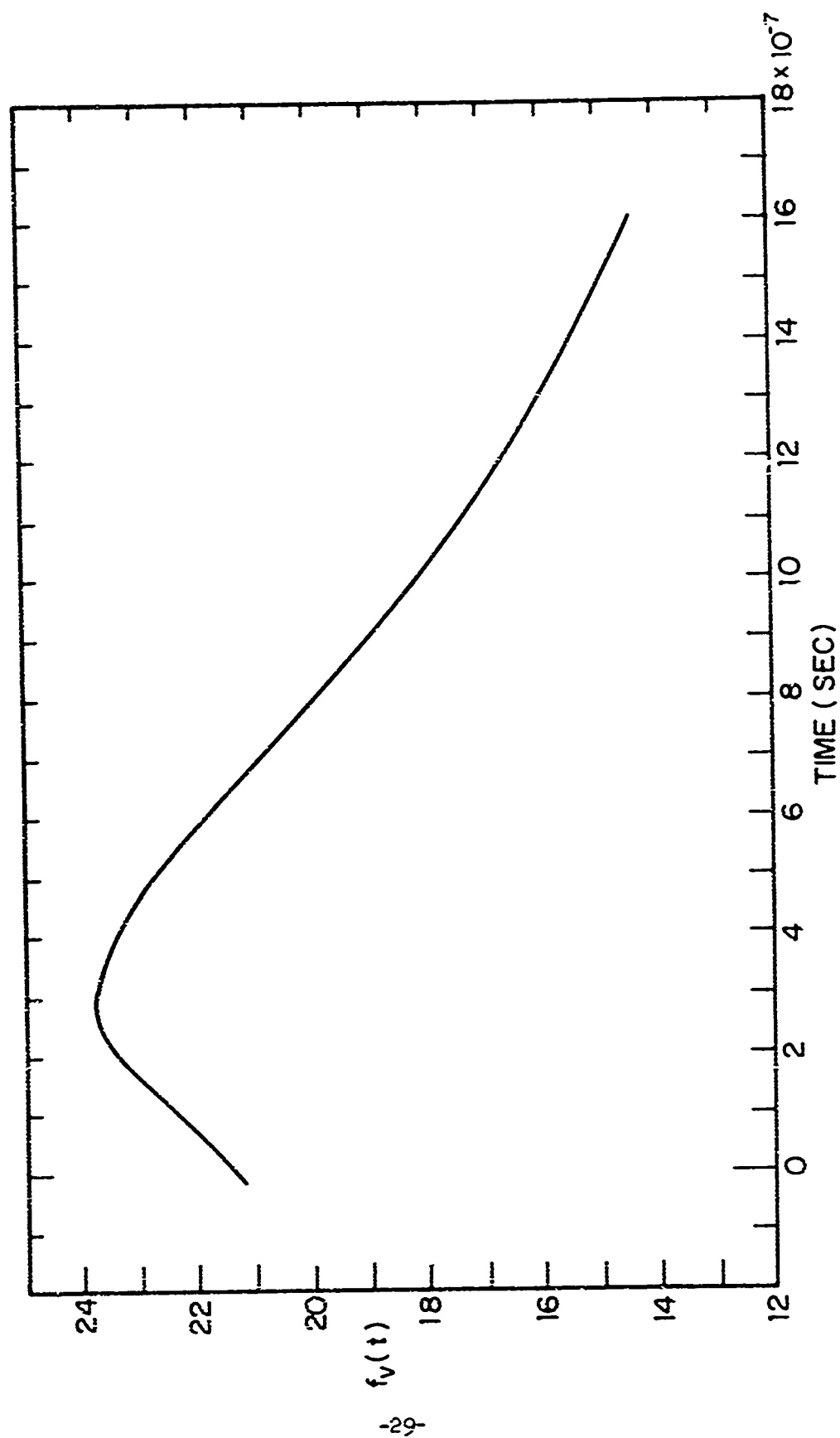


Fig. 7. Theoretical pressure time history for a viscous medium.

References

1. A. Silbiger, Focusing of Sound and Explosive Pulses in the Ocean, Cambridge Acoustical Associates, Inc. Tech. Rept. U-286-188, ONR Contract N00014-66-C-0110, June 1968.
2. R. M. Barash and J. A. Goertner, Refraction of Underwater Explosion Shock Waves: Pressure Histories Measured at Caustics in a Flooded Quarry, U.S. Naval Ordnance Laboratory Tech. Rept. 67-9, 19 April 1967.
3. R. J. Urick, Principles of Underwater Sound for Engineers, McGraw-Hill Book Co., New York, 1967, pp 72-74.
4. Silbiger, op. cit., p. 25, Eq. 48.
5. Urick, op. cit., p. 87.
6. R. Thrun, U.S. Naval Ord. Lab., private communication.
7. Silbiger, op. cit., p. 28.
8. Urick, op. cit., p. 72.
9. P. M. Morse and K. U. Ingard, Theoretical Acoustics, McGraw-Hill Book Co., New York, 1968, p. 282, Eq. 6.4.22.; and
F. R. Norwood, "Propagation of Transient Sound Signals into a Viscous Fluid," J. Acoust. Soc. Am. 44, 450-457 (1968), Eq. 1.

Unclassified
Security Classification

DOCUMENT CONTROL DATA - R & D		
(Security classification of title, body of abstract and indexing annotation must be entered when the overall report is classified)		
1. ORIGINATING ACTIVITY (Corporate author) CAMBRIDGE ACOUSTICAL ASSOCIATES, INC. 129 Mt. Auburn Street Cambridge, Massachusetts 02138		23. REPORT SECURITY CLASSIFICATION Unclassified
2. REPORT TITLE UNDERWATER SHOCKWAVE FOCUSING AT CAUSTICS: Comparison of Theory and Experiment		24. GROUP -----
4. DESCRIPTIVE NOTES (Type of report and inclusive dates) Final Report 1 July 1968 - 31 August 1969		
5. AUTHOR(S) (First name, middle initial, last name) David A. Sachs		
6. REPORT DATE 31 August 1969	7a. TOTAL NO. OF PAGES 30	7b. NO. OF REFS 9
8a. CONTRACT OR GRANT NO. N00014-66-C 0110		9a. ORIGINATOR'S REPORT NUMBER(S) U-322-186
b. PROJECT NO. NR 321-002		
10. DISTRIBUTION STATEMENT Qualified requestors may obtain copies of this report from DDC.		
11. SUPPLEMENTARY NOTES		12. SPONSORING MILITARY ACTIVITY Field Projects Branch, Office of Naval Research Washington, D. C.
13. ABSTRACT <p>A theory of shockwave focusing is employed in an attempt to predict the extent of focusing of explosive pulses at caustics as observed experimentally.</p> <p>Assuming a viscous medium and a physically reasonable model for the explosive pulse, an order of magnitude comparison with experiment is obtained. The omission of viscosity from the mathematical model leads to unacceptably large amplification at the caustic.</p>		

DD FORM 1473

REPLACES DD FORM 1473, 1 JAN 64, WHICH IS OBSOLETE FOR ARMY USE.

Unclassified
Security Classification

Unclassified
Security Classification

14. KEY WORDS	LINK A		LINK B		LINK C	
	ROLE	WT	ROLE	WT	ROLE	WT
Wave propagation Underwater Sound Transmission Caustics Shockwaves Underwater Explosions						

Unclassified

Security Classification